AD-A172 784

DTIC FILE COPY

THE EFFECT OF DUST MODELS ON GLOBAL NUCLEAR WINTER

THESIS

Philip Q. Pontier
Captain, USAF

AFIT/GNE/ENP/86M-11

DISTRIBUTION STATEMENT A
Approved for public release;
Distribution Unlimited

DEPARTMENT OF THE AIR FORCE
AIR UNIVERSITY
AIR FORCE INSTITUTE OF TECHNOLOGY

Wright-Patterson Air Force Base, Ohio

PII Redacted

86 10 10 082

86 10 10 082

AFIT/GNE/ENP/86M-11

THE EFFECT OF DUST MODELS ON
GLOBAL NUCLEAR WINTER

THESIS

Philip Q. Pontier
Captain, USAF

AFIT/GNE/ENP/86M-11

Approved for public release; distribution unlimited

AFIT/GNE/ENP/86M-11

THE EFFECT OF DUST MODELS ON GLOBAL NUCLEAR WINTER

THESIS

Presented to the Faculty of the School of Engineering

of the Air Force Institute of Technology

Air University

In Partial Fulfillment of the

Requirements for the Degree of

Master of Science in Nuclear Engineering

Philip Q. Pontier, B.S.

Captain, USAF

March 1986

Table of Contents

List of Figures

List of Tables

Abstract

A series of optical depth calculations were accomplished to assess the effects of various existing dust and soot models on the transmission of incident sunlight. A change in the standard deviation of the particle size distribution from two to four, assuming constant total density, resulted in a decrease in the visible optical depth by a factor of ten.

A technique using a method of direct integration was developed for the calculation of the effective optical depth of nuclear induced dust and soot clouds. Contributions from directly transmitted photons, first scattered photons using anisotropic cross-sections, and all subsequently scattered photons were used to calculate the amount of light transmitted through the cloud. Absorption effects were also included.

The results of this study were comparable to the results of several recent nuclear winter studies.

THE EFFECT OF DUST MODELS ON

GLOBAL NUCLEAR WINTER

I. Introduction

Background

Many scientists have expressed growing concern over the climatic effects of a nuclear war. Large amounts of soot and dust injected into the upper atmosphere may absorb and reflect large enough amounts of solar radiation for a prolonged enough period of time that the surface temperature of the planet could be affected. The low temperature along with toxic smog and radioactivity following a nuclear war have become known as "nuclear winter" (Turco et al., 1983a:33).

Past studies in this area (NRC, 1985; Ramaswamy and Kiehl, 1985; Turco et al., 1983a) have calculated the light levels and temperatures following a nuclear exchange for a variety of scenarios. Some of the more extreme scenarios predict light levels below the limits of photosynthesis and temperature drops of up to 30° C.

The optical properties of a nuclear cloud depend on a variety of factors. For example, total dust mass, index of refraction, composition, total area covered, height and thickness of the cloud are a few of the important factors which need to be determined. Many generally accepted values for these parameters exist and have been used in the previous studies. But the one factor which has received little or no consideration is the sensitivity of the particle size distribution of the cloud on the nuclear winter effect.

Purpose

The purpose of this study is to examine the effect of particle size distribution and cloud composition on the attenuation of solar radiation due to a nuclear cloud.

Approach

The cloud was assumed to be a semi-infinite cloud instantaneously distributed over the region of interest. Vertically the cloud is modeled as a series of horizontal layers where each individual layer is homogeneous and contains the appropriate fraction of the total mass lofted. The Air Force Geophysics Laboratory's Mie Scattering computer code, MIE3 (Blatner, 1972), was used to calculate the absorption and scattering coefficients of the nuclear cloud. This code was modified slightly to enable it to run on the ASD Cyber computer here at WPAFB. Further modifications were incorporated to produce an abbreviated output file containing a table of scattering and extinction coefficients for the different layers of the cloud. These values were then used by the computer code SCAT (see the appendix) to calculate the fraction of visible sunlight transmitted through the cloud. This code uses a method of direct integration which accounts for anisotropic and multiple scattering.

An alternative method of calculating optical coefficients was also investigated. The Mie scattering subroutine of MIE3 was replaced with a subroutine using Diermendjian's formulas for extinction (Diermendjian, 1969:29). The accuracy of this approximation was then determined by comparison to the results obtained using Mie theory.

Overview

Chapter II of this report contains a brief discussion of extinction and optical cross-sections. The method of direct integration is developed in Chapter III. Chapter IV describes the different types of dust and soot clouds used for the calculations. The results are listed in Chapter V and Chapter VI is a discussion of the results. A summary and list of recommendations are contained in Chapter VII. Included as an appendix is a description and listing of the computer code SCAT.

II. Theory

Extinction

The interaction of sunlight as it passes through a nuclear cloud consists of two processes, scattering and absorption. The two processes are additive and their sum is referred to as extinction.

Scattering. When incident light is scattered by a dust particle, the particle becomes a point source of the scattered energy. This energy is reradiated into the total solid angle around the particle. A photon can therefore be scattered in any direction and the scattering continues until the photon is lost out of the top or bottom of the cloud or until it is absorbed. The light reaching the ground is therefore a combination of the directly transmitted light, neither scattered nor absorbed, and the downward scattered light. This type of transmission is referred to as diffuse transmission (McCartney, 1976:33).

Absorption. The absorptive properties of a cloud are determined by the refractive index of the medium. The index of refraction consists of a real and imaginary part, sometimes referred to as the scattering index and absorption index respectively (McCartney, 1976:225). A highly absorptive particle will have a large imaginary index, such as

0.66 which is typical for carbon. A less absorptive particle, such as soil, will have a much smaller absorptive index such as 0.001 (Ackerman and Toon, 1981:3362).

Cross-Sections

Mie theory, developed by Gustav Mie in 1908, and Diermendjian's approximation provide two means of computing the optical cross-section of a particle. An efficiency factor, Q, is computed which relates the geometric cross-section of a particle to its optical cross-section (McCartney, 1976:221). The microscopic cross-section is then found by the relation

$$\sigma = Q\pi r^2 \tag{1}$$

where

σ = microscopic cross-section

r = particle radius

For a polydispersion such as a nuclear cloud the microscopic cross-sections are integrated across the particle size distribution to find the average macroscopic cross-section, β, of the cloud. Using Equation (1) we obtain

$$\beta = \pi \int r^2 Q n(r)\, dr \tag{2}$$

where

β = macroscopic cross-section

$n(r)$ = particle size distribution

The computer code MIE3 performs these calculations and provides macroscopic cross-sections for extinction, scattering and absorption. These cross-sections are more commonly known as the optical coefficients β_e, β_s, and β_a respectively and have units of inverse length.

Angular Coefficients. The coefficients computed by the above method measure the ability of the medium to scatter and absorb light but they do not indicate the direction in which the light will scatter. Mie scattering exhibits several maxima and minima in the scattered intensity as a function of scattering angle. The positions of these maxima depend upon particle size and wavelength of the incident light (Scott, 1982:1021).

Angular scattering coefficients may be obtained by introducing the angular distribution function $f(\theta)$, which is the fraction of scattered radiation directed into a unit solid angle in the direction of θ (Chu et al., 1975:ix). The angular distribution functions can be represented in the following form,

$$f(\theta) = \frac{1}{4\pi} \sum_{n=0}^{\infty} a_n P_n(\cos\theta) \qquad (3)$$

where

P_n = Legendre polynomials,

a_n = angular distribution coefficients, and

θ = planar scattering angle measured from an extension of the initial direction

The angular distribution coefficients are a function of wavelength, particle size and index of refraction and are listed in Chu et al. (1957). The infinite sum in Equation (3) can usually be terminated after 10 to 15 terms for most of the particle sizes of interest in a nuclear cloud. Representative values of $f(\theta)$, from Equation (3), are listed in Table I to show the scattering pattern of visible light (λ = .5 μm) from dust particles of three different radii.

Combining $f(\theta)$ with β_s gives an angular scattering coefficient $\beta_s(\theta)$ where

$$\beta_s(\theta) = f(\theta)\beta_s \tag{4}$$

Two limitations of this method may be important depending on the composition of the cloud.

1. Unless a large data base is used and values of $f(\theta)$ are integrated over the entire size distribution, an average $f(\theta)$ must be computed from some average particle size. This may be acceptable for a narrow size distribution but should be used with caution on a wider size distribution.

2. The coefficients, a_n, in Equation (3) are based on non-absorbing particles. They can be used with good accuracy when the extinction index is less than 0.001 but should not be used with highly absorptive materials such as

TABLE I

ANGULAR DISTRIBUTION FUNCTIONS

Angle (Degrees)	f(θ) r=.1	f(θ) r=.25	f(θ) r=1
0	.18	.81	5.75
10	.18	.75	2.60
20	.17	.59	.17
30	.15	.40	.08
40	.13	.23	.08
50	.11	.11	.06
60	.09	.04	.04
70	.08	.02	.04
80	.07	.01	.02
100	.05	.01	.02
120	.05	.01	.01
140	.06	.01	.01
160	.07	.01	.06
180	.07	.01	.05

soot (Chu et al., 1957:ix). When calculations involving soot are desired, using $f(\theta) = 1/4\pi$ is a good estimate since soot particles have radii ranging from 0.01 to 0.1 μm and symmetric scattering can be assumed (McCartney, 1976:21; Broyles, 1985:330).

Optical Depth

Optical depth, τ, is a nondimensional number used to describe the cumulative depletion that a beam of light experiences as it travels through a medium (Pittock et al., 1985:309). In terms of the optical coefficient of a homogeneous medium, the optical depth is

$$\tau = \beta z \tag{5}$$

where z is the path length. The transmittance is then calculated using

$$T = \exp(-\tau) \tag{6}$$

An optical depth of one then reduces the beam to e^{-1} (i.e., 37 percent) of its original value.

The term optical depth, sometimes called direct or extinction optical depth, is used to refer to removal by both scatter and absorption. Other forms of optical depth are often used and refer to the process by which the light is removed. These include scatter optical depth, τ_s, and absorption optical depth, τ_a. The form which is most often used in nuclear winter calculations is the effective optical depth, τ_{eff}. This form accounts for all the light which eventually finds its way out of the bottom of the cloud. It includes both directly transmitted and downward scattered light.

III. Method

The method of direct integration used in this study to calculate the effective optical depth of a nuclear cloud, when scattering is significant, is adapted from the work done by Robertson (1968). Robertson demonstrated that the accuracy of this method approaches that of Monte Carlo calculations for the transport of X-ray photons in matter. The procedure used by Robertson is outlined here along with the modifications made to adapt it to visible light photons in dust cloud calculations.

Geometry

Figure 1 shows the geometry of the semi-infinite dust cloud. An arbitrary target column is selected and divided into equally sized mesh cells of thickness Δz and diameter Δz. Each mesh cell of the target column is encircled by an infinite number of concentric tori having a radial thickness of Δz and a cross-sectional area of Δz^2. Each torus acts as a source kernel which will emit scattered photons toward the target column. Field points are located at the geometric center of each cell and will serve as reference points for the calculation of photon fluence. A field point is also placed at the bottom of the target column; the fluence at this point will be used to calculate the effective optical depth.

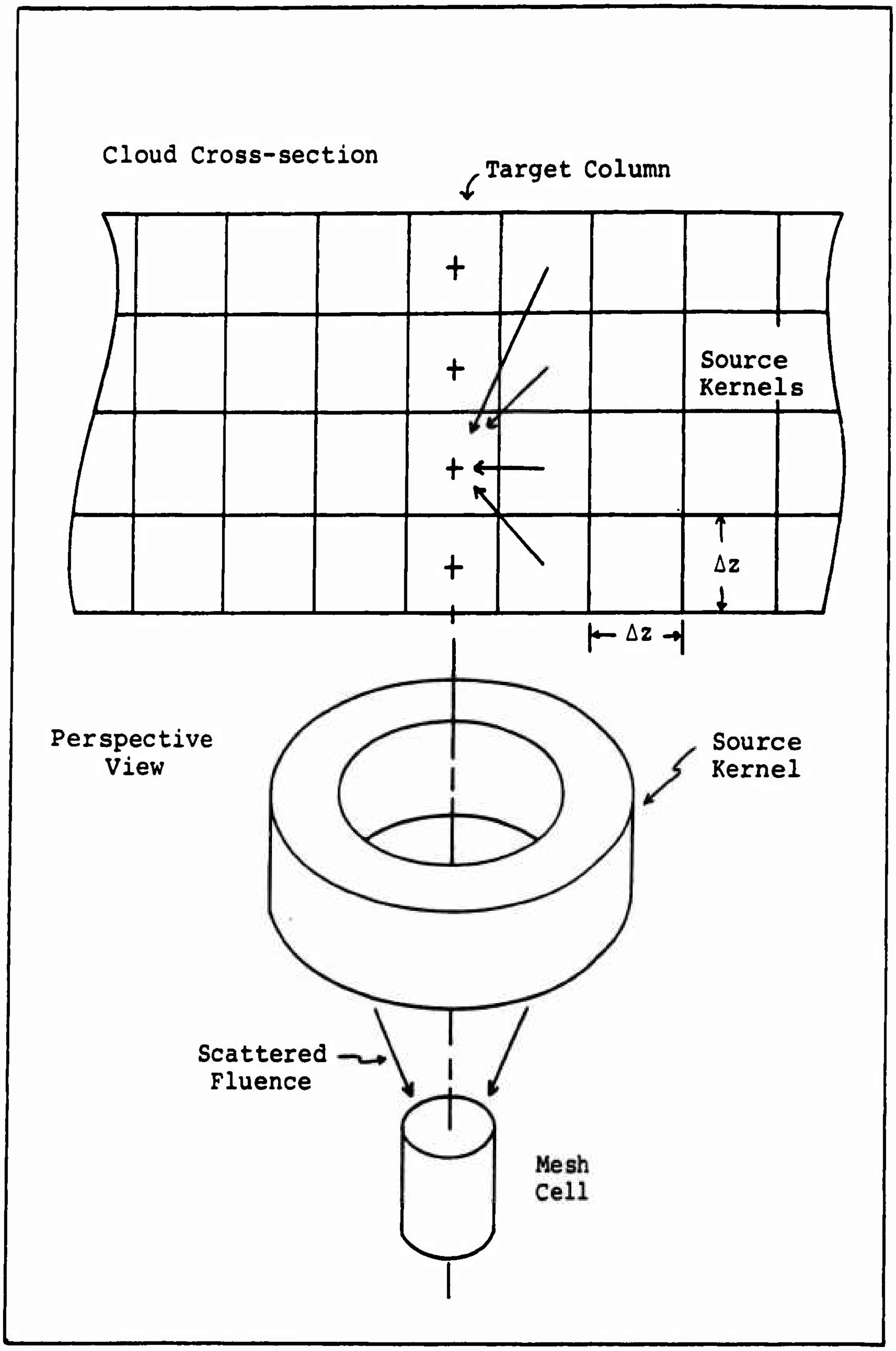

Fig. 1. Cloud Geometry

Assumptions

1. The photon fluence at any field point is the same as the mean fluence across the cell.

2. Anisotropic scatter is used on the first scatter only. All subsequent scatters are assumed isotropic.

3. Scatterers are spherical in shape and uniform in density.

4. Sunlight is assumed to have a wavelength of 0.5 μm.

5. Scattered photons are emitted from the point sources located along the toric center line of each source kernel.

6. Extinction and scattering coefficients remain constant throughout each horizontal subdivision of the cloud.

Direct Fluence

The direct fluence reaching a given point along the target column is calculated using pure extinction.

$$\phi_i^0 = \phi^0 \exp\left[-\sum_{j=1}^{L} \beta_e^j \, r_j\right] \tag{7}$$

where

ϕ_i^0 = direct fluence at point i (photons/m^2)

ϕ_0 = incident fluence (photons/m^2)

β_e^j = extinction coefficient for mesh cell j

L = number of mesh cells encountered between top of cloud and point i

r_j = distance traveled in mesh cell j

The extinction optical depth can now be calculated by using the direct fluence reaching the last field point. Using Equation (6)

$$\tau = \ln(T) \tag{8}$$

where

$T = \phi_{bot}/\phi_0$

ϕ_{bot} = fluence at the last field point

<u>First Scatter</u>

Scattered photons, originating from the volume of air surrounding the target column, add to the fluence of the target column. The contribution from a single source kernel to the fluence at a given field point is

$$d(\phi_j) = \phi_i \beta_s^i f(\theta) \exp\left[-\sum_{k=i}^{j} r_k \beta_e^k\right] \frac{dVol}{R^2} \tag{9}$$

where

$d(\phi_j)$ = fluence reaching field point j from dVol

ϕ_i = fluence in source kernel i

β_s^i = scattering coefficient in source kernel i

$f(\theta)$ = fraction of scattered radiation directed toward field point j
use Eq. (3) for first scatter
use $1/4\pi$ for all other scatters

r_k = distance traveled through region k

β_e^k = extinction coefficient for region k

R = distance from source kernel i to field point j

dVol = volume of source kernel i

In a semi-infinite cloud, the fluence in any source kernel will be identical to the fluence in the corresponding mesh cell of the target column. Therefore the direct fluence calculated at each of the field points of the target column become the source terms for Equation (9).

The total contribution of first scattered photons reaching a given field point is found by integrating Equation (9).

$$\phi_j = \int_{Vol} d(\phi_j) \tag{10}$$

Point kernel integration is used starting with the innermost column of source kernels and continuing outward until some rejection criteria is met. The integration is then repeated for each of the field points in the target column.

Second and Subsequent Scatters

The fluence of first scattered photons reaching the target column now become the source terms in Equation (9) for the second scatter calculation. The second scattered fluence will become the source for the third and so on until the contribution becomes negligible.

Effective Optical Depth

To compute optical depth we must know the number of photons per unit area arriving at the last field point. A source kernel which is offset from the target column does not "see" the same area as a source directly over the last field point (Figure 2). For this reason a correction factor of $\cos\theta$ must be applied to Equation (9) when computing the fluence at the last field point.

The effective optical depth of the cloud can then be calculated using the relation

$$\tau_{eff} = \ln\left[\frac{\phi_B}{\phi_0}\right] \tag{11}$$

where ϕ_B is the sum of the direct and all the scattered fluence reaching the last field point at the bottom of the cloud.

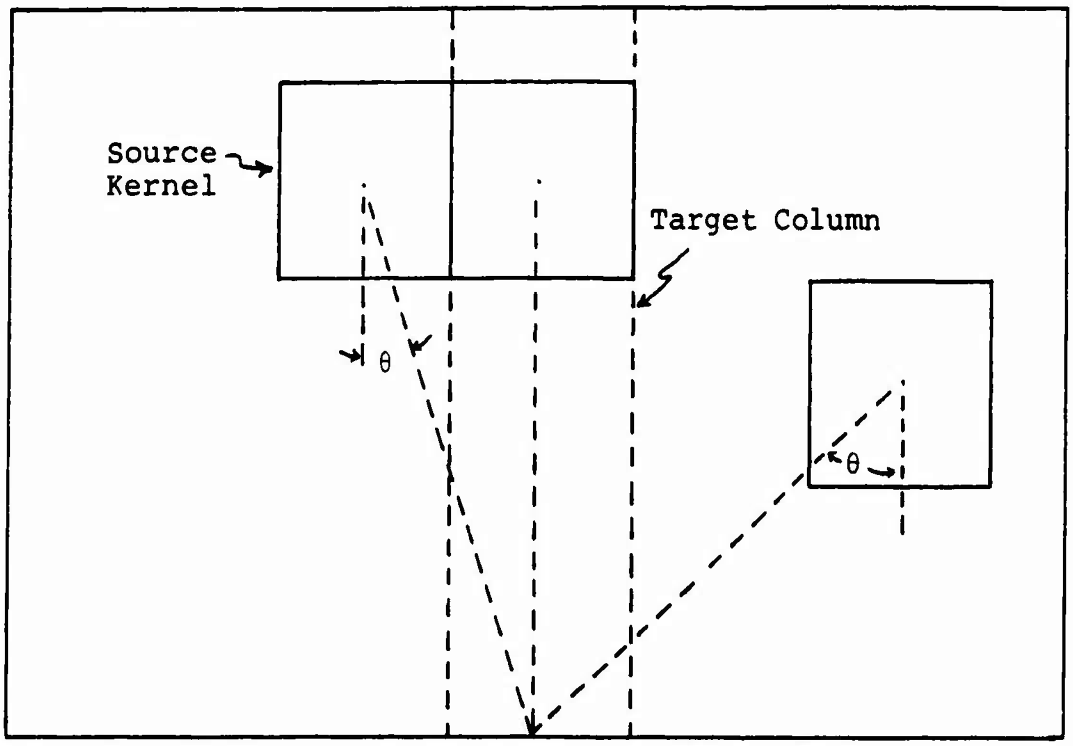

Fig. 2. Cloud Bottom as Seen from Source Kernel

IV. Cloud Models

The dust cloud chosen for this study was suggested by Turco et al. (1983b:7) as a likely product of a massive nuclear exchange. The total yield expended consisted of a combination of surface, near-surface and low air bursts totaling 9400 megatons. A total of 1.5×10^{12} g of dust was lofted with a height dependent injection profile shown in Figure 3. A cloud area of 1.1×10^{8} km^2 was assumed which represents the region of the earth's surface between 30° and 70° north latitude. The optical properties of the dust cloud were based on a refractive index of 1.5-.001i and a density of 2500 kg/m^3.

The soot cloud, in Figure 3, results from the large-scale urban and forest fires ignited during the attack. This cloud was used as the base case for the NRC (1985:82) study and contains a total mass of 0.18×10^{12} g with an area of 2.5×10^{8} km^2 covering the entire northern hemisphere. The soot has an index of refraction of 1.5-.1i and a density of 1000 kg/m^3.

Four representative particle size distributions were selected for this study and are listed in Table II. The three dust distributions were selected to test the sensitivity of optical depth to the distribution parameters. The soot distribution was chosen to investigate the impact of a highly absorptive medium.

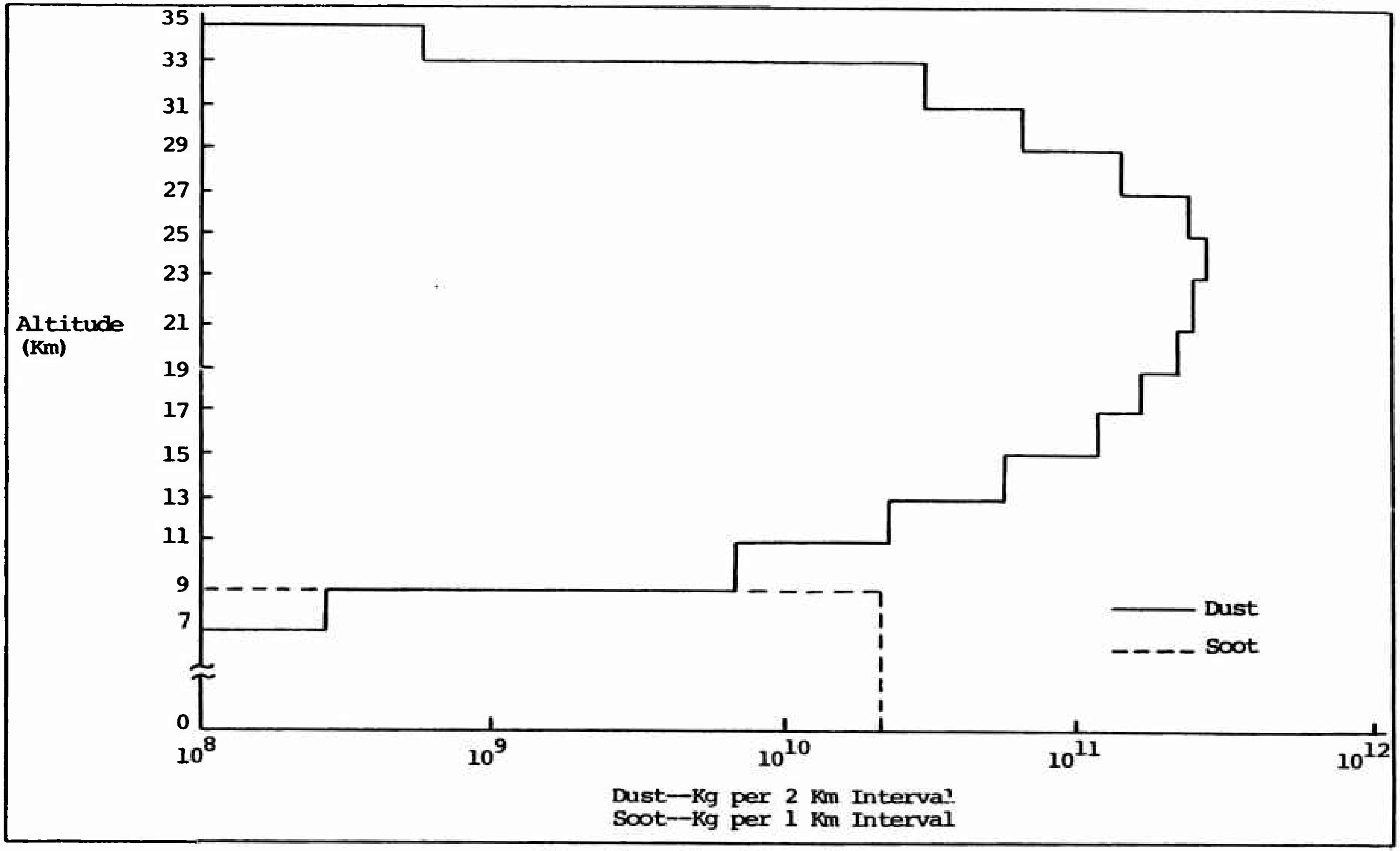

Fig. 3. Cloud Profile

TABLE II

PARAMETERS FOR PARTICLE SIZE DISTRIBUTIONS

Name	r (μm)	σ	α	Remarks
TTAPS-Dust	0.25	2	4	Log Normal with Power Law Tail (Turco et al., 1983b:21)
DELFIC-Dust	0.204	4	-	Log Normal (Conners, 1985:11)
NCAR-A-Dust	1.65	2.2	-	Log Normal (Patterson, 1977:2080)
NRC-Soot	0.1	2	-	Log Normal (NRC, 1985:82)

r = mean radius

σ = standard deviation

α = exponent of power tail

The three dust particle size distributions were all normalized to the same total mass density. The total mass of 1.5 x 10^{12} g was distributed as shown in Figure 3 and the mass density computed for each cloud layer. These mass densities were then used in the three dust distributions for the optical depth calculations.

V. Results

Optical depth calculations, using the cloud models described in the previous chapter, were made for each of the four particle size distributions. The incident light was assumed to be visible sunlight with a fixed wavelength of 0.5 μm. The mesh cell size chosen for the integration was one kilometer for dust and one-half kilometer for soot. This represented a distance of approximately one-fifth and one-half of the shortest mean free path respectively. Angular scattering coefficients, from Equation (3), were calculated using the mean radius of the particle size distribution.

Integration and scattering calculations were halted when the contribution from the next iteration represented less than 1 percent of the total fluence. This convergence criteria required integration out to approximately 35 kilometers and included from two to eight scatters for the dust clouds. The more absorbent soot cloud only required calculations out to seven kilometers with three scatters.

Tables III and IV list the results of these calculations. Table III compares the accuracy of Diermendjian's approximation to that of Mie theory for both extinction and scattering optical depth. The results of the multiple scattering calculations used to compute effective optical depth are listed in Table IV.

TABLE III

DIRECT OPTICAL DEPTH

Cloud Model	Removal Process	Optical Depth Mie	Optical Depth Diermendjian	% Error
TTAPS Dust	τ_e	2.42	2.34	3
	τ_s	2.35	2.30	2
DELFIC Dust	τ_e	0.24	0.23	4
	τ_s	0.21	0.21	0
NCAR-A Dust	τ_e	1.00	0.96	4
	τ_s	0.89	0.88	1
NRC Soot	τ_e	3.94	3.82	3
	τ_s	2.52	2.79	11

The extinction optical depth is listed along with the optical depth which results after each successive scatter until the rejection criteria is met. Table IV was calculated using the Mie coefficients. Diermendjian's approximation produced similar results with errors ranging from 5 to 7 percent.

TABLE IV

EFFECTIVE OPTICAL DEPTH

Number of Scatters	Particle Size Distribution			
	TTAPS Dust	NCAR-A Dust	NRC Soot	DELFIC Dust
Direct	2.42	1.00	3.94	0.24
1	1.70	0.86	3.80	0.12
2	1.50	0.80	3.73	0.11
3	1.38	0.77	3.70	"
4	1.31	0.76	"	"
5	1.26	0.75	"	"
6	1.23	"	"	"
7	1.21	"	"	"
8	1.20	"	"	"

VI. Discussion

This chapter deals with four main topics: (1) the characteristics of the cloud and how they effect optical depth, (2) the validity of the basic assumptions used in the calculations, (3) comparison of the results to previous work, and (4) the accuracy of Diermendjian's formulas.

Cloud Characteristics

The main characteristic of a dust cloud which is altered by varying the particle size distribution parameters is the number concentration of submicron particles (i.e. $0.1 < r < 1$ μm). Submicron particles are extremely efficient scatterers with optical cross-sections that can be as much as 4.4 times larger than their geometric cross-sections (McCartney, 1976:248).

The TTAPS dust and NRC soot clouds are characterized by very narrow size distributions with high concentrations of submicron particles. In comparison the DELFIC dust and NCAR dust clouds use distributions with a much lower fraction of small particles. This lower concentration results from the larger standard deviation of the DELFIC distribution and the larger mean radius of the NCAR distribution.

The impact of these submicron particles can be seen by comparing the optical depths listed in Table III. The three dust clouds show the sensitivity of optical depth to the distribution parameters. Comparison of the TTAPS and DELFIC dust results indicates that the standard deviation is the most sensitive parameter. An increase in standard deviation by a factor of two decreases the optical depth by a factor of ten. The NCAR dust distribution has approximately the same standard deviation as the TTAPS but the mean radius is larger by a factor of six; this also decreases the optical depth but not to such a great extent. Although a direct comparison of the dust and soot is not possible, due to the different refractive indices, the trend toward high scattering efficiencies can be seen in both the TTAPS dust and NRC soot distributions.

The results listed in Table IV indicate that the number of scatters which must be considered is also affected by the cloud properties. The cloud's scattering efficiency and absorptive index will determine how much light is scattered and the rate at which this scattered light is attenuated. The source terms, used to calculate the scattered contribution to the total fluence, originate from the fraction of light scattered out of the direct beam. Both the NRC soot and TTAPS dust clouds scatter approximately 91 percent of the incident light and therefore have relatively large source terms compared to the DELFIC dust cloud which only scatters 21 percent of the incident light. The scattered light in the soot cloud is quickly attenuated, after only three scatters, due to the highly absorptive nature of the soot. In the dust cloud, however, less than 1 percent of the light is absorbed and the light continues to scatter until spherical divergence becomes a factor. As a result of this scattering the optical depth of the dust cloud is reduced by as much as 50 percent, while in the soot cloud the scattered light is unable to make a significant contribution and only reduces the optical depth by 6 percent.

Validity of Assumptions

The basic assumption of a semi-infinite cloud proved to be very good. The integration in the radial direction converged in from one-half to seven mean free paths. The soot cloud required integration to seven kilometers which represents approximately seven mean free paths. Convergence in the less turbid clouds occurred in less than one mean free path due to the small amount of scattered light combined with the effects of spherical divergence.

The photon fluence as calculated in Equation (7) was a good approximation of the mean fluence across the cell. In all but the soot cloud a cell thickness of one kilometer could be used. The shorter mean free path in the NRC soot cloud required a cell thickness of one-half kilometer to keep the error below 1 percent.

To test the validity of calculating the angular scattering coefficients using the mean radius of the distribution an attempt was made to bracket the correct answer. The two extremes would be the use of a very small radius and a very large radius as the basis for the angular scattering. A small radius would reduce the amount of forward scattering and tend to increase the optical depth since more light is being scattered up and away from the source column. The larger radius would also tend to increase the optical depth, since the extreme forward scattering permits only those source kernels directly adjacent to the target column to scatter light into the column. Since both extremes yield optical depths greater than the true optical depth we can use this as an upper limit. These calculations were performed using the TTAPS dust cloud with radii of 0.1 μm and 1 μm giving optical depths of 1.39 and 1.59 respectively. To find the lower limit several calculations were performed using radii between 0.1 μm and 1 μm and a minimum value of 1.19 was found using a radius of 0.18 μm. The actual optical depth should therefore have a value between 1.19 and 1.39. Using the mean radius of the size distribution a value of 1.20 was obtained. Similar calculations were done using the DELFIC dust cloud and the minimum, mean radius and maximum optical depths were 0.11, 0.11 and 0.15 respectively. The actual optical depth can therefore be approximated with fairly good accuracy by using the mean radius for angular scattering.

One last assumption to be considered is the use of isotropic scatter on all scatters after the first. In all but the TTAPS dust cloud the direct and first scattered fluence accounted for over 90 percent of the transmitted fluence. Considering the small contribution from second and subsequent scatters and the difficulty in tracking the direction of each scatter, the use of isotropic scattering is not a bad assumption.

Previous Work

Both the TTAPS dust and NRC soot clouds were used as the basis for nuclear winter calculations in previous studies. Turco et al. (1983b) used the TTAPS cloud as a baseline scenario and reported an effective optical depth of 1.4, whereas 1.20 was found here. A radiative transfer model, developed by Sagan and Pollock (1976), was used as an approximation to account for the combined effects of multiple scattering and absorption. Their model does not use specific scattering angles but instead uses a single factor to account for the fraction of light scattered in the forward direction. The different approach to angular scattering used in this study may account for the slight variation in results.

The NRC study reported an extinction optical depth of 4.0 for their baseline smoke cloud (NRC, 1985:84). This compares favorably with the extinction optical depth of 3.94 that was calculated in this study.

Diermendjian's Approximation

Diermendjian's formulas provide a simple alternative means of calculating optical efficiencies. The results listed in Table III show that this method is accurate to within 4 percent for most cases. Larger errors have been reported (Broyles, 1985:328) when the index of refraction exceeds 1.5-.25i. This may become a factor for soot and smoke cloud calculations which typically involve imaginary indices of 0.1 to 0.6.

VII. Summary and Recommendations

Summary

A method of computing the effective optical depth of a nuclear cloud was developed. The method uses direct integration, anisotropic and multiple scattering to determine the fraction of incident light which emerges from the bottom of the cloud. The results of this method are comparable to the results obtained in previous nuclear winter studies.

A comparative study was performed to determine the effect of particle size distribution parameters on the nuclear winter phenomenon. It was found that the standard deviation of the distribution was the most sensitive factor. An increase in the standard deviation by a factor of two can decrease the optical depth by a factor of ten.

The relationship between the impact of multiple scattering and cloud composition was also investigated. The absorptive properties of the cloud played an important role in determining the reduction in optical depth due to multiple scattering. For a nonabsorptive dust cloud the optical depth can be reduced by as much as 50 percent, but in a more absorptive soot cloud the reduction was only 6 percent.

Recommendations

Future investigations of the nuclear winter phenomenon should include a study of the time dependent aspects of optical depth. These should include sedimentation, agglomeration, rainout and horizontal diffusion. Diermendjian's formulas could be used in place of the lengthy Mie scattering code, and provide a simple and fairly accurate means of recalculating optical coefficients as the cloud properties change with time.

To reduce the overall uncertainties in nuclear winter calculations, the physical and optical properties of dust and soot should be more accurately defined.

Appendix: Computer Program Listing (SCAT)

The following pages contain a listing of the computer program SCAT used for the calculation of the effective optical depth of a nuclear cloud. The program is written in FORTRAN IV and will run on the ASD CYBER computer.

```
      PROGRAM SCAT (INPUT,OUTPUT,TAPE9,TAPE7,TAPE5=INPUT,TAPE6=OUTPUT)

      DIMENSION BEX(20),BSC(20),BE(100),BS(100),F0(100),F1(100)
C
C     PROGRAM COMPUTES EFFECTIVE OPTICAL DEPTH OF AN AEROSOL CLOUD
C     USES ANISOTROPIC SCATTER ON FIRST SCATTER ONLY ALL OTHER
C     SCATTERS ARE ASSUMED ISOTROPIC
C
C     USER SETS LIMITS OF INTEGRATION, INTEGRATION INCREMENT AND
C     NUMBER OF SCATTERS
C
C     VARIABLES DEFINED BY USER
C           KTHICK: CLOUD THICKNESS (KM)
C            KSLAB: THICKNESS OF CLOUD LAYERS (KM)
C            NDIST: RADIAL DISTANCE TO WHICH INTEGRATION IS TO
C                   BE ACCOMPLISHED (KM),DISTANCE=NDIST*KDZ
C            NSCAT: NUMBER OF SCATTERS TO BE USED
C              KDZ: INTEGRATION INCREMENT (KM)
C
C           INPUT FROM TAPE9
C                  TAPE9 SHOULD CONTAIN (KTHICK/KSLAB) SETS OF
C                  EXTINCTION AND SCATTERING COEFFICIENTS (KM**-1)
C                  FORMAT(2E15.5)
C
C     DERIVED VARIABLES
C           NCOEFF: NUMBER OF COEFFICIENT SETS TO BE READ FROM TAPE9
C              NDZ: NUMBER OF INTERNAL FIELD POINTS
C             KBOT: NUMBER TO DEFINE LAST FIELD POINT
C            COSIN: COSINE OF SCATTERING ANGLE
C                R: DISTANCE BETWEEN SOURCE AND FIELD POINT
C             FTOT: TOTAL FLUENCE AT LAST FIELD POINT
C
C           OUTPUT IS WRITTEN TO TAPE7
C
C     ** DEFINE CLOUD **
      KTHCK=28
      KSLAB=2
      KDZ=1
      NDIST=35
      NSCAT=11
      NCOEFF=KTHICK/KSLAB
      NDZ=KTHICK/KDZ
      KBOT=NDZ+1
C
C     ** READ COEFFICIENTS FROM TAPE9 **
      READ(9,100) (BEX(J),BSC(J),J=1,NCOEFF)
```

```
C     ** DIVIDE CLOUD INTO NDZ LAYERS AND ASSIGN EXTINCTION**
C     ** AND SCATTERING COEFFICIENTS TO EACH LAYER          **
      INC=KSLAB/KDZ
      I=0
      K=INC
      DO 20 L=1,NCOEFF
            II=I+L
            KK=K+L
            DO 10 N=II,KK
                  BE(N)=BEX(L)
                  BS(N)=BSC(L)
 10         CONTINUE
            I=I+INC
            K=K+INC
 20   CONTINUE
C
C     ** INITIALIZE ARRAYS **
      DO 30 N=1,KBOT
            F0(N)=0.0
            F1(N)=0.0
 30   CONTINUE
      BE(KBOT)=0.0
      BS(KBOT)=0.0
C
C     ** COMPUTE DIRECT FLUENCE **
      F0(1)=EXP(-BE(1)*KDZ/2.)
      DO 40 N=2,NDZ
            F0(N)=F0(N-1)*EXP(-(BE(N-1)+BE(N))*KDZ/2.)
 40   CONTINUE
      F0(KBOT)=F0(KBOT-1)*EXP(-BE(KBOT-1)*KDZ/2.)
      FTOT=F0(KBOT)
C
      WRITE(7,200) NDIST*KDZ,KDZ
      WRITE(7,300)
      WRITE(7,400)
      WRITE(7,500) F0(KBOT),ALOG(F0(KBOT))
C
C     ** INTEGRATE OVER VOLUME OF CLOUD **
      DO 85 NS=1,NSCAT
      DO 75  L=1,NDIST
      DO 70  N=1,KBOT
            IF (N .EQ. KBOT) A=KDZ/2.
            IF (N .NE. KBOT) A=0.0
            DO 65 M=1,NDZ
               R=SQRT((L*KDZ)**2+((M-N-A)*KDZ)**2)
               COSIN=((N-M-A)*KDZ)/R
C
```

```
C           ** COMPUTE EXTINCTION (R2) BETWEEN SOURCE M AND CELL N **
               IF (M .EQ. N) R2=BE(N)*KDZ*L
               IF (M .EQ. N) GO TO 60
               R2=0.0
               IF (M .GT. N) GO TO 50
               DO 45 K=M,N
                  R1=FLOAT(KDZ)
                  IF (K .EQ. M .OR. K .EQ. N) R1=KDZ/2.
                  R2=R2+R1*BE(K)/ABS(COSIN)
 45            CONTINUE
               GO TO 60
 50            DO 55 K=N,M
                  R1=FLOAT(KDZ)
                  IF (K .EQ. N .OR. K .EQ. M) R1=KDZ/2.
                  R2=R2+R1*BE(K)/ABS(COSIN)
 55            CONTINUE
 60            CONTINUE
C
C              ** COMPUTE SCATTERED FLUENCE ARRIVING AT CELL N **
               F=F0(M)*BS(M)*L*KDZ**3*EXP(-R2)/(2.*R**2)
               IF (N .EQ. KBOT) F=F*COSIN
               IF (NS .EQ. 1)   F=F*FRAC(COSIN)
               F1(N)=F1(N)+F
 65         CONTINUE
 70   CONTINUE
 75   CONTINUE
      FTOT=FTOT+F1(KBOT)
      WRITE(7,600) F1(KBOT),NS,ALOG(FTOT)
      DO 80 N=1,KBOT
      F0(N)=F1(N)
      F1(N)=0.0
 80   CONTINUE
 85   CONTINUE
      WRITE(7,400)
      WRITE(7,700) FTOT
 100  FORMAT(2E15.5)
 200  FORMAT(I5,* KM*,8X,*DZ=*,I3/)
 300  FORMAT(10X,*%FLUX*,4X,*SOURCE*,8X,*OPTICAL DEPTH*)
 400  FORMAT(9X,*-------------------------------------*)
 500  FORMAT(F15.5,5X,*DIRECT*,3X,F15.5)
 600  FORMAT(F15.5,2X,I3,*SCATTER*,F15.5)
 700  FORMAT(F15.5,4X,*TOTAL*)
      STOP
      END
```

```
C
C
C
      FUNCTION FRAC(COSIN)
      DIMENSION A(26),P(26)
C
C     COMPUTES ANGULAR DISTRIBUTION FUNCTION
C           COSIN: COSINE OF SCATTERING ANGLE
C               P: LEGENDRE POLYNOMIALS
C               A: ANGULAR DISTRIBUTION COEFFICIENTS
C              NA: THE NUMBER OF COEFFICIENTS BEING USED
C           ALPHA: 2*PI*R/WAVELENGTH
C
C     ** DATA FOR ALPHA=1       USE NA=5 **
C     DATA A/1.0,.59685,.56415,.10955,.00902/
C
C     ** DATA FOR ALPHA=3       USE NA=11 **
C     DATA A/1.0,2.203,2.58189,2.18461,1.34801,.56111,.21739,
C    $       .04954,.0083,.00107,.00012/
C
C     ** DATA FOR ALPHA=10      USE NA=26 **
      DATA A/1.0,2.22873,3.38409,3.78255,4.76483,5.16916,5.70666,
     $       5.89478,5.92665,5.875,5.41723,5.11591,4.30744,
     $       3.77023,2.78576,2.14168,1.13952,.86443,.61407,
     $       .61738,.76154,.48723,.62348,-.09834,.00737,.00203/
C
      NA=26
      FRAC=0.0
      P(1)=1.0
      P(2)=COSIN
      DO 20 N=3,NA
            P(N)=(P(N-1)*(2*N-3)*COSIN-P(N-2)*(N-2))/(N-1)
 20   CONTINUE
      DO 30 N=1,NA
            FRAC=FRAC+A(N)*P(N)
 30   CONTINUE
      RETURN
      END
```

Bibliography

Ackerman, T. P. and O. B. Toon. "Absorption of Visible Radiation in Atmospheres Containing Mixtures of Absorbing and Nonabsorbing Particles," Applied Optics, 20: 3661-3667 (October 1981).

Blattner, W. Utilization Instructions for Operation of the Mie Programs on the CDC-6600 Computer at AFCRL. Contract F19628-70-C-0156. Radiation Research Associates, Inc., Fort Worth TX, October 1972.

Broyles, A. A. "Smoke Generation in a Nuclear War," American Journal of Physics, 53: 323-332 (April 1985).

Chu, C. et al. Tables of Angular Distribution Coefficients for Light-Scattering by Spheres. Ann Arbor: University of Michigan Press, 1957.

Conners, S. P. Aircrew Dose and Engine Dust Ingestion from Nuclear Cloud Penetration. MS Thesis, Air Force Institute of Technology (AU), Wright-Patterson AFB OH, 1985.

Diermendjian, D. Electromagnetic Scattering on Spherical Polydispersions. New York: American Elsevier Publishing Company, 1969.

McCartney, Earl J. Optics of the Atmosphere. New York: John Wiley and Sons, Inc., 1976.

National Research Council (NRC). The Effects on the Atmosphere of a Major Nuclear Exchange. Washington DC: National Academy Press, 1985.

Patterson, E. M. and D. A. Gillette. "Commonalities in Measured Size Distributions for Aerosols Having a Soil Derived Component," Journal of Geophysical Research, 82: 2074-2082 (May 1977).

Pittock, A. B. et al. Environmental Consequences of Nuclear War. New York: John Wiley and Sons, Inc., 1985.

Ramaswamy, V. and J. T. Kiehl. "Sensitivities of the Radiative Forcing Due to Large Loadings of Smoke and Dust Aerosols," Journal of Geophysical Research, 90: 5597-5613 (June 1985).

Robertson, W. R. The Calculation of Photon Transport in Slab Geometries by a Method of Direct Integration. MS Thesis, Air Force Institute of Technology (AU), Wright-Patterson AFB OH, 1968.

Sagan, C. and J. B. Pollack. "Anisotropic Nonconservative Scattering and the Clouds of Venus," Journal of Geophysical Research, 72: 469-477 (1967).

Scott, J. F. "Scattering of Electromagnetic Radiation," McGraw-Hill Encyclopedia of Physics, edited by Sybil P. Parker. New York: McGraw-Hill, Inc., 1983.

Turco, R. P. et al. "Nuclear Winter: Global Consequences of Multiple Nuclear Explosions," Science, 222: 1283-1292 (December 1983)a.

-----. Global Atmospheric Consequences of Nuclear War. Interim Report, R&D Associates, Marina Del Rey CA (March 1983)b.

VITA

Captain Philip Pontier [redacted] PII Redacted

[redacted], New Jersey. He graduated from high school in Franklin Lakes, New Jersey in 1972 and attended Grove City College, Grove City, Pennsylvania from which he received the degree of Bachelor of Science in Mechanical Engineering in May 1976. He completed Undergraduate Navigator Training and received his wings in July 1977. He then served as a KC-135 navigator and instructor navigator in the 509th Air Refueling Squadron at Pease AFB, New Hampshire. In 1982 he was assigned to the 42nd Air Refueling Squadron at Loring AFB, Maine as an evaluator navigator. He entered the School of Engineering, Air Force Institute of Technology, in August 1984.

Permanent address: [redacted] PII Redacted

UNCLASSIFIED

SECURITY CLASSIFICATION OF THIS PAGE

AD-A172 784

REPORT DOCUMENTATION PAGE

1a. REPORT SECURITY CLASSIFICATION UNCLASSIFIED	1b. RESTRICTIVE MARKINGS
2a. SECURITY CLASSIFICATION AUTHORITY	3. DISTRIBUTION/AVAILABILITY OF REPORT Approved for public release; distribution unlimited
2b. DECLASSIFICATION/DOWNGRADING SCHEDULE	
4. PERFORMING ORGANIZATION REPORT NUMBER(S) AFIT/GNE/ENP/86M-11	5. MONITORING ORGANIZATION REPORT NUMBER(S)
6a. NAME OF PERFORMING ORGANIZATION School of Engineering	6b. OFFICE SYMBOL (If applicable) AFIT/ENP
7a. NAME OF MONITORING ORGANIZATION	
6c. ADDRESS (City, State and ZIP Code) Air Force Institute of Technology Wright-Patterson AFB, OH 45433	7b. ADDRESS (City, State and ZIP Code)
8a. NAME OF FUNDING/SPONSORING ORGANIZATION	8b. OFFICE SYMBOL (If applicable)
9. PROCUREMENT INSTRUMENT IDENTIFICATION NUMBER	
8c. ADDRESS (City, State and ZIP Code)	10. SOURCE OF FUNDING NOS.

PROGRAM ELEMENT NO.	PROJECT NO.	TASK NO.	WORK UNIT NO.

11. TITLE (Include Security Classification)
See Box 19

12. PERSONAL AUTHOR(S)
Philip Q. Pontier, BS, Capt, USAF

13a. TYPE OF REPORT	13b. TIME COVERED	14. DATE OF REPORT (Yr., Mo., Day)	15. PAGE COUNT
MS Thesis	FROM ______ TO ______	1986 March	48

16. SUPPLEMENTARY NOTATION

17. COSATI CODES

FIELD	GROUP	SUB. GR.
04	01	

18. SUBJECT TERMS (Continue on reverse if necessary and identify by block number)
Nuclear Clouds, Atmospheric Scattering, Dust Clouds, Nuclear Winter

19. ABSTRACT (Continue on reverse if necessary and identify by block number)

Title: THE EFFECT OF DUST MODELS ON GLOBAL NUCLEAR WINTER

Thesis Chairman: Charles J. Bridgman, Ph.D.
Professor of Nuclear Engineering
Department of Engineering Physics

Abstract continued on reverse.

Approved for public release: IAW AFR 190-1/.
Lynn E. Wolaver 9 May 86
LYNN E. WOLAVER
Dean for Research and Professional Development
Air Force Institute of Technology (ATC)
Wright-Patterson AFB OH 45433

20. DISTRIBUTION/AVAILABILITY OF ABSTRACT UNCLASSIFIED/UNLIMITED ☒ SAME AS RPT. ☐ DTIC USERS ☐	21. ABSTRACT SECURITY CLASSIFICATION UNCLASSIFIED

22a. NAME OF RESPONSIBLE INDIVIDUAL	22b. TELEPHONE NUMBER (Include Area Code)	22c. OFFICE SYMBOL
Charles J. Bridgman, Ph.D.	(513) 255-4498	AFIT/ENP

DD FORM 1473, 83 APR EDITION OF 1 JAN 73 IS OBSOLETE.

UNCLASSIFIED

SECURITY CLASSIFICATION OF THIS PAGE

A series of optical depth calculations were accomplished to assess the effects of various existing dust and soot models on the transmission of incident sunlight. A change in the standard deviation of the particle size distribution from two to four, assuming constant total density, resulted in a decrease in the visible optical depth by a factor of ten.

A technique using a method of direct integration was developed for the calculation of the effective optical depth of nuclear induced dust and soot clouds. Contributions from directly transmitted photons, first scattered photons using anisotropic cross-sections, and all subsequently scattered photons were used to calculate the amount of light transmitted through the cloud. Absorption effects were also included.

The results of this study were comparable to the results of several recent nuclear winter studies.